

## Appendix A: List of Preforms

- Preforms listed in italics represent those that are part of the development sequence of the random hole optical fiber.
- Preforms listed in bold indicate those that were fabricated using one of the crucible techniques.

1999:	
DK 99-01	Quartz holey fiber
DK 99-02	Overclad of CQ1
DK 99-03	Overclad of CQ1
DK 99-04	Pyrex™ Holey Fiber
DK 99-05	Pyrex™ Holey Fiber
DK 99-06	Pyrex™ Holey Fiber
2000:	
DK 00-01	LIP and Pyrex™ holey fiber
DK 00-02	LIP and Pyrex™ holey fiber
DK 00-03	LIP and Pyrex™ holey fiber
DK 00-04	Pyrex™ hexagonal holey fiber
DK 00-05	Silica hexagonal holey fiber
<i>DK 00-06</i>	<i>Sol-gel powder preform</i>
<b>DK 00-07</b>	<b>Simple Pyrex™ tube with LIP</b>
<b>DK 00-08</b>	<b>LIP in thick walled silica tube</b>

DK 00-09	<i>Sol-gel powder preform</i>
DK 00-10	Silica Hex with LIP
DK 00-11	Silica Hex with hollow core for LIP (never inserted)
DK 00-12	MCVD Borosilicate/Germanosilicate
DK 00-13	MCVD PM 1
DK 00-14	MCVD PM 2
DK 00-15	MCVD PM3
2001:	
<b>DK 01-01</b>	<b>LIP Crucible</b>
<i>DK 01-02</i>	<i>Aerogel without silica tube</i>
<i>DK 01-03</i>	<i>Aerogel chunks in silica tube</i>
<i>DK 01-04</i>	<i>Sol-gel powder preform</i>
DK 01-05	Silica cane holey preform
<b>DK 01-06</b>	<b>LIP Crucible</b>
<i>DK 01-07</i>	<i>Sol-gel powder preform</i>
<i>DK 01-08</i>	<i>White Microbubble Preform</i>
<i>DK 01-09</i>	<i>Purple Microbubble Preform</i>
<i>DK 01-10</i>	<i>Aerogel (single piece w/ core) preform</i>
<i>DK 01-11</i>	<i>Microbubble preform w/ silica disk spacers</i>
<i>DK 01-12</i>	<i>Aerogel preform w/ silica spacers</i>
DK 01-13	MCVD W profile preform
<i>DK 01-14</i>	<i>33% Microbubble/ground silica preform</i>

DK 01-15	Ground silica preform
DK 01-16	10% Microbubble preform
DK 01-17	1% Silicon carbide preform
DK 01-18	1% Silicon carbide preform
2002:	
<b>DK 02-01</b>	<b>Kigre MM2™ Crucible</b>
DK 02-02	1% Silicon nitride w/ 325-mesh silica sealed at vacuum
DK 02-03	1% Silicon carbide w/ 325-mesh silica (w/ vacuum but not sealed)
DK 02-04	Pure 325-mesh silica sealed at vacuum
DK 02-05	Pure 100-mesh silica (w/ vacuum but not sealed)
	All subsequent preforms containing silica use the 100-mesh silica
DK 02-06	0.5% Silicon nitride w/ 100-mesh silica
DK 02-07	0.5% Silicon nitride w/ 100-mesh silica
DK 02-08	0.25% Silicon nitride w/100-mesh silica
DK 02-09	0.1% Silicon nitride w/100-mesh silica
DK 02-10	0.05% Silicon nitride
DK 02-11	0.05% Silicon nitride
DK 02-12	0.025% Silicon nitride
DK 02-13	0.075% Silicon nitride
DK 02-14	0.04% Silicon nitride

DK 02-15	0.075% Silicon nitride
DK 02-16	0.06% Silicon nitride
DK 02-17	0.075% Silicon nitride (19x25)
DK 02-18	0.075% Silicon nitride (13x19)
DK 02-19	0.05% Silicon nitride (13x19)
DK 02-20	0.075% Silicon nitride with Gold (9x15)
DK 02-21	0.074% Silicon nitride (13x19)
DK 02-22	0.083% Silicon carbide
DK 02-23	0.075% Silicon nitride w/ Synthetic silica core
DK 02-24	0.065% Silicon nitride w/ Synthetic silica core
DK 02-25	0.15% Silicon nitride which has been pre-heated in a furnace to 1000°C for 45 min (1 hr ramp up) w/ Synthetic silica core
2003:	
DK 03-01	0.1% Silicon nitride (same treatment as DK02-25) w/ synthetic silica core
<b>DK 03-02</b>	<b>Tellurium Oxide in silica</b>
DK 03-03	0.065% silicon nitride core preform
<b>DK 03-04</b>	<b>Tellurium Oxide in Pyrex™</b>
DK 03-05	MCVD Pure Germania core preform
<b>DK 03-06</b>	<b>F2™ Glass in silica crucible</b>
<b>DK 03-07</b>	<b>Tellurium Oxide in Pyrex™ pre-melted</b>
<b>DK 03-08</b>	<b>F2™ Glass in Pyrex™</b>

<b>DK 03-09</b>	<b>Tellurium Oxide in Pyrex™ pre-melted</b>
2004:	
<b>DK 04-01</b>	<b>Pyrex™ in Silica Crucible</b>
<b>DK 04-02</b>	<b>Pyrex™ in Silica Crucible</b>
<b>DK 04-03</b>	<b>Schott F2™ in Simax™ (Suction Crucible)</b>
<b>DK 04-04</b>	<b>Schott SFL6™ in Simax™ (Suction Crucible)</b>
<b>DK 04-05</b>	<b>Schott SFL6™ in Silica (Suction Crucible)</b>
<b>DK 04-06</b>	<b>Fisk “Sample 3” in Simax™ (Suction Crucible)</b>
<b>DK 04-07</b>	<b>Fisk “Sample 3” in Simax™ (Suction Crucible)</b>
<b>DK 04-08</b>	<b>GeO<sub>2</sub> in Silica (Suction Crucible)</b>
<b>DK 04-09</b>	<b>GeO<sub>2</sub> in Silica</b>

Selected preforms fabricated with others:

With Ismael Torres	
PCF 1 (IT 03-01)	Ordered Hole Fiber (OHF) (Cobweb Style)
PCF 2 (IT 03-02)	Ordered Hole Fiber
PCF 3 (IT 03-03)	OHF (Cobweb Style)
PCF 4 (IT 03-04)	OHF (Cobweb Style)
PCF 5 (IT 03-05)	Photonic Crystal Fiber
PCF 6 (IT 03-06)	Photonic Crystal Fiber/OHF
With Chris Rose	

CJR 02-02	Large Core OHF
CJR 02-03	Large Core OHF
CJR 02-04	Cobweb OHF
CJR 02-11	Ordered Hole Fiber
CJR 02-12	Double Clad Fiber (Germanium/Ytterbium doped core with OHF outer clad)

## **Appendix B: General Operation of a Fiber Draw Tower**

The process of drawing optical fibers is generally the same between different draw towers. Minor variations in the components, particularly in the coating system, are common. A preform is fed into a furnace from the top while fiber is drawn out of the bottom of the furnace and then down through a series of components before ultimately being spooled. A schematic of the fiber draw tower used for this work can be seen in Figure 52.

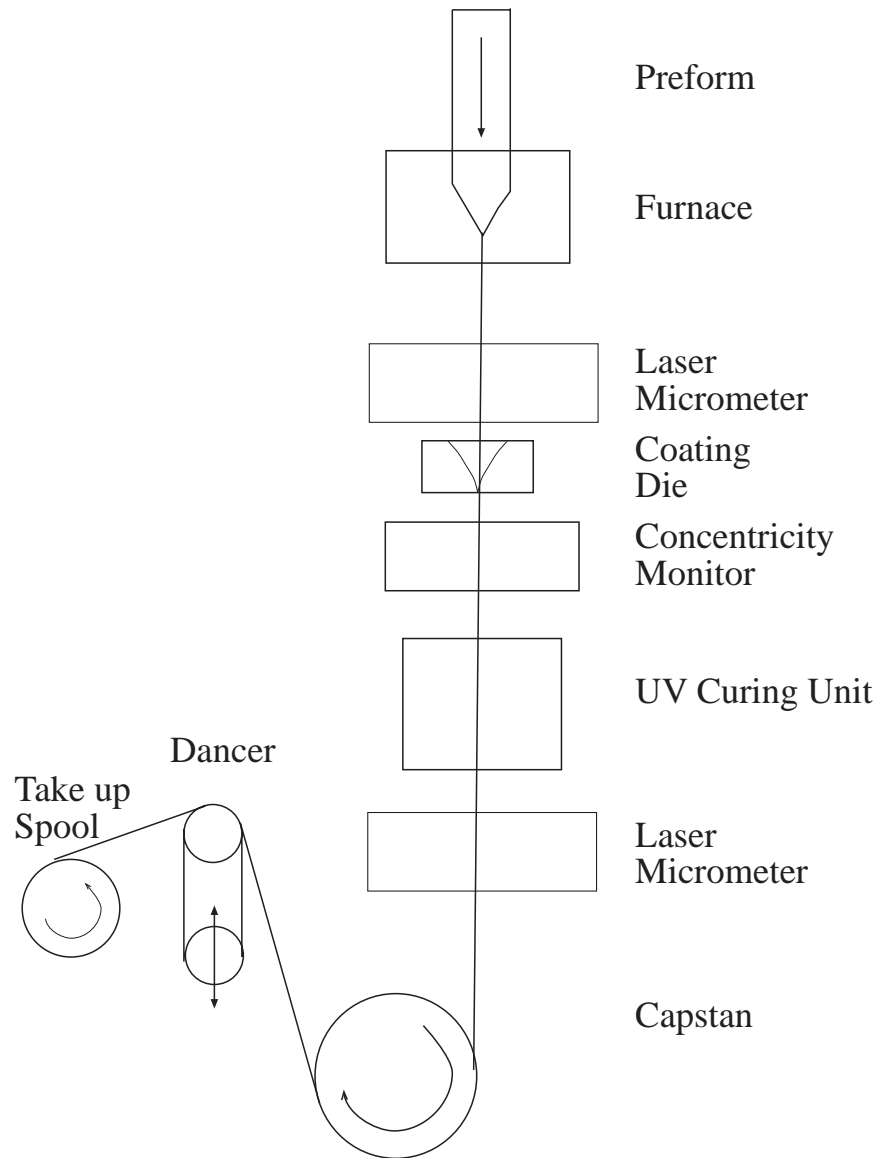


**Figure 52: Draw Tower Layout**

The preform is lowered into the furnace by a stepper motor capable of drive speeds with increments of 0.01 mm/min. The fiber is drawn out of the furnace by the capstan at speeds ranging from 10 to 80 cm/sec. By controlling the speed at which preform enters the furnace and the speed at which the fiber is drawn out of the furnace the diameter of the finished fiber can be determined, nearly

independent of the furnace temperature. The relation between the two is based, in most cases, on a simple conservation of volume. The diameters of the fiber, both bare and coated, are measured with laser micrometers.

Once the fiber is past the capstan, a dancer arm and take up spool work in concert to spool the fiber at the same rate as the draw speed.

### ***Furnace***

The graphite resistive element furnace is operated with AC current, with a power consumption of approximately twelve kilowatts. It is cooled with a 400 gallon water ballast tank, and a purified argon supply is used to prevent oxidation of the element.

The hot zone of the furnace is the region of highest temperature. A number of factors impact the size of the hot zone of the furnace, including size of the heating element, and whether the furnace has a one piece or two piece liner. The one piece liner, which was used in this work, results in a somewhat larger hot zone with a smoother temperature profile than the two piece liner. Near the center of the furnace the profile is roughly parabolic. Using a C-type thermocouple, the hot zone of the furnace was profiled to determine the heat distribution. The results of this profile can be seen in Figure 53. Although the absolute values of temperature will change with both time and peak temperature, the general trends will remain the same.

The temperature profile which is given in Figure 53 is based on a measurement which was made with only the thermocouple within the furnace. When there is a preform in the furnace, its presence will alter the heat distribution. There are two mechanisms by which the preform will alter the heat distribution. Firstly, the conduction of heat through the glass. Secondly, there is a continuous exposure of lower temperature material at the upper regions of the hot zone since the preform is being continuously lowered into the furnace.

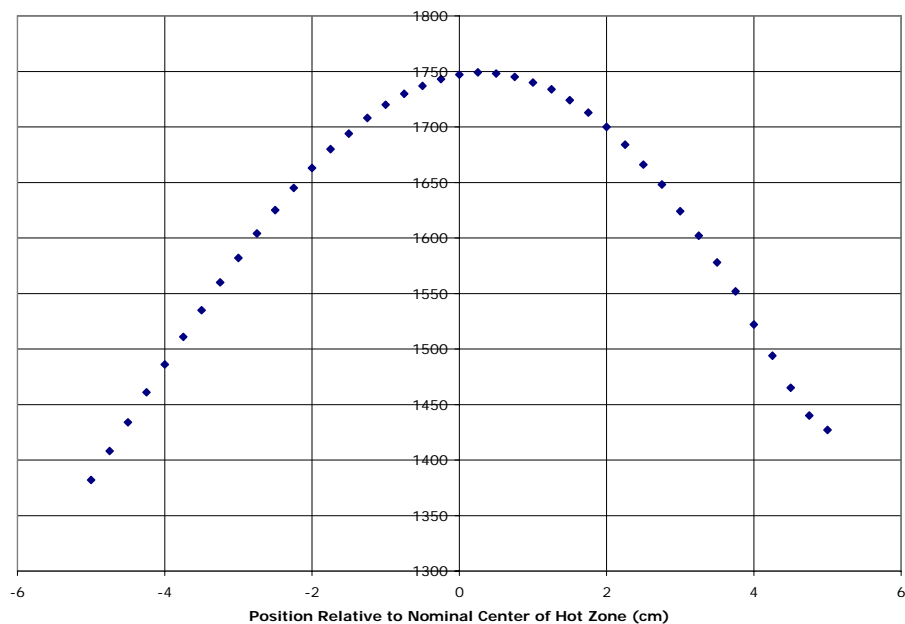


**Figure 53: Temperature Profile of Astro Furnace**

The temperature of the furnace drops off quite rapidly to either side of the hottest region of the furnace. Although defining the width of the hot zone is somewhat arbitrary, I would estimate its width as being approximately 2.5 cm.

### **Effect of Furnace Properties on the Drawing of Holey fibers**

One of the issues which was encountered in the drawing of holey fibers (of the ordered set, rather than the random) was that variations in the draw tension across the preform resulted in fibers which were strongly dissimilar from the preform geometry. The phenomena which were observed included:

- Variations of tension of the draw over time (occasionally varying from near zero to approximately one kilogram of tension in the space of five minutes)
- Apparent variations in the malleability of the glass between different portions of the cross section of the preform, resulting in collapse of half of the hole structure while the other half is well preserved.

One of the parameters of the draw which could cause such effects is the choice of the purge gas which is used to surround the preform inside the resistive element furnace. In general, the denser the gas that is used, the more of the energy is transferred conductively to the preform rather than radiatively. As a result, if one wishes for optimal conduction transfer, one would use, in order of decreasing efficiency, Nitrogen, Argon, and then Helium.

### ***Coating System***

One of the necessary treatments of the fiber during the draw is the application of a polymer coating to the fiber, which serves to protect the natural strength of the fiber. The coating prevents abrasion as well as eliminates the weakening associated with exposure to moisture and dust. The coating used on the draw

tower is Desolite™ polyurethane acrylate, an ultraviolet cured polymer.

The coating is applied with a pressurized split die system, with a diameter of 330  $\mu\text{m}$ . The die can be aligned along four axes (two translation, and two rotation). After being coated, the fiber passes through a concentricity monitor, then is cured in a UV unit. The concentricity monitor operates by diffracting a laser beam around the fiber and coating, and then imaging that pattern with a pair of video cameras.

## Appendix C: Measurement of Refractive Index Profiles

In order to measure the refractive indices of the various materials which are incorporated into the fibers, a new technique needed to be implemented. The reason for this is that the normal method of doing such a measurement would be to measure the angle of divergence of a multimode section of the fiber, and thereby, determine the relationship between the core and cladding indices. This mechanism breaks down however, if the index difference becomes excessively high. The reason is that the high index drop at the output face of the fiber has its own critical angle for total internal reflection, and one can end up with modes which are supported but are unable to be coupled out of the fiber end face. Due to the extreme index differences, in some cases as large as 0.4, it was necessary to build a reflectometer to measure the refractive index of the materials.

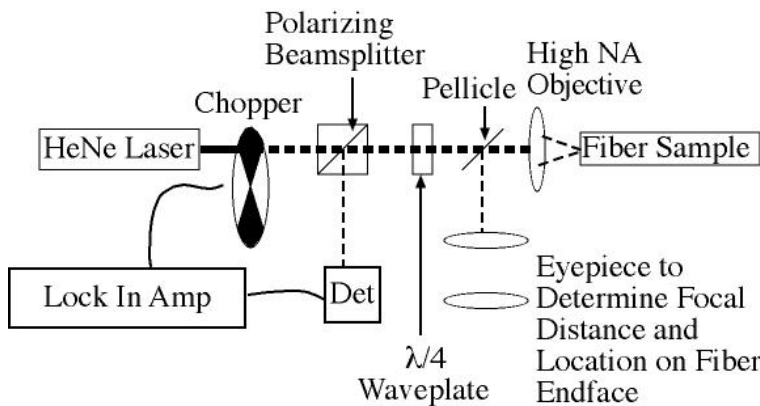


**Figure 54: Layout of Refractive Index Reflectometer**

A schematic of the reflectometer can be seen in Figure 54. A linearly polarized Helium Neon laser is passed through a chopper, and then through a polarizing beam splitter. Then, after passing through a quarter wave plate to render the

light circularly polarized, the light is focused onto the endface of the fiber. On retro-reflection the signal is recollimated, and, on passing through the quarter wave plate a second time, is again linearly polarized orthogonally to the original polarization. Thus, when it reaches the polarizing beam splitter, it is reflected to the output face, and arrives at a pin photodetector. This signal, along with a reference, are fed into an EG&G lock-in amplifier. In addition, a small portion of the light which is retro-reflected from the endface of the fiber, is diverted by a pellicle. This light is passed through a 6x microscope objective to form a real image. After attenuation, a fiber inspection microscope is used to magnify this image, allowing the operator to determine the precise location on the fiber endface which is being probed.

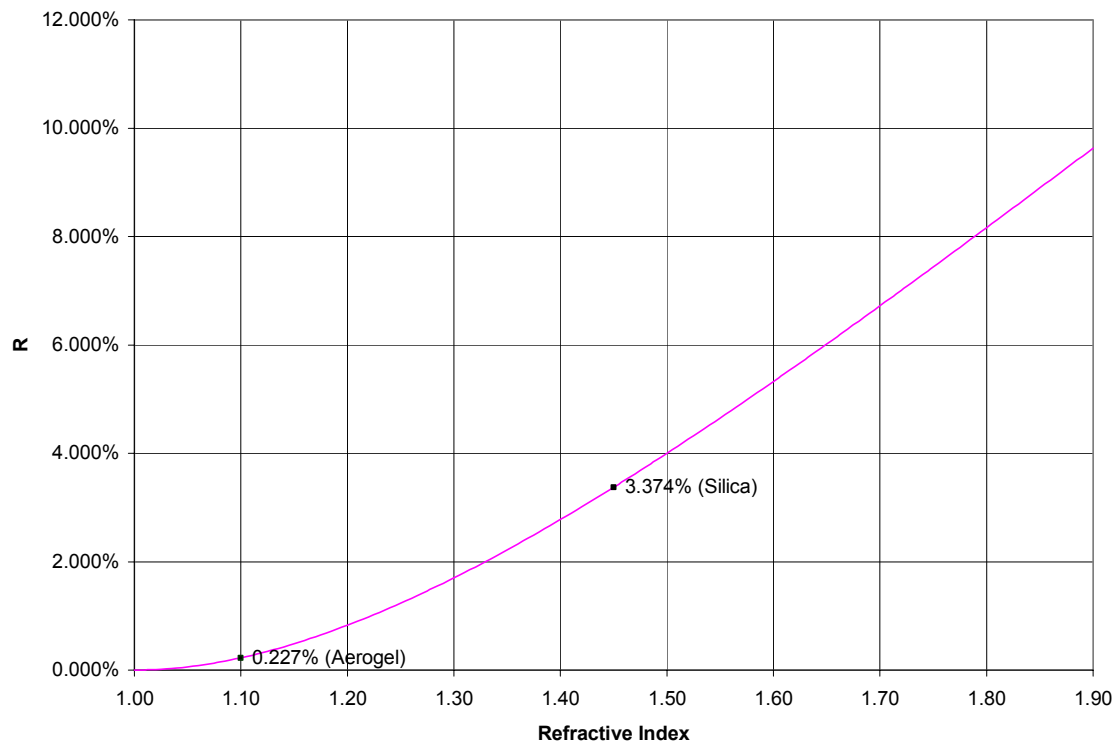


**Figure 55: Prediction of Power Reflection Percentages as a Function of Refractive Index**

By comparing the strength of the reflected signal from a region which is comprised of bulk fused silica (with a known index of 1.45702 at the helium/neon wavelength of 633 nm), it is possible to obtain refractive index values, based on the power reflectivity relation. In Figure 55 one can see the power reflection profile which is derived from this dependence on the refractive index shown in Equation 10.

$$R = \frac{(n_2 - n_1)^2}{(n_2 + n_1)^2}$$

**Equation 10: Fresnel Reflection Coefficient**

Values obtained for the refractive index of the claddings included those measured for fibers which were derived from aerogel cladding (preform DK01-03), with an index of 1.10. Measurements were also made for fibers made from mixed microbubble/crushed fused silica cladding. This technique is also to be applied to the core of the LIP-based fibers.

## *Curriculum Vita*

### **Daniel Kominsky**

#### **Education:**

Spring 1999-2005:

Doctoral Student, Department of Material Science and Engineering, Virginia Tech.

Dissertation: *Development of Random Hole Optical Fiber and Crucible Technique Optical Fibers* Advisors: Dr. R.H. Stolen and Dr. Gary Pickrell.

Fall 1995-Fall 1998:

M.S. in Optics, University of Rochester, Rochester, NY. Advisor: Dr. S.N. Houde-Walter.

Fall 1991-Spring 1995:

B.A. Vassar College, Poughkeepsie, NY. Double Major in Physics and Astronomy with a Minor in Mathematics. Graduated with general honors as well as departmental honors in both majors. Advisor: Dr. D. Elmegreen.

#### **Professional Work Experience:**

Summer 2004-Present:

Research Scientist and Aeropulsion Business Unit Manager at Prime Research, LC.

Spring 1999- Summer 2004:

Graduate Research Assistant in the fiber fabrication facility at Virginia Tech.

Responsibilities include being the primary operator of the fiber fabrication systems, including preform lathes and fiber draw towers. Built and maintained preform fabrication facilities, as well as developing safety guidelines for all aspects of fiber fabrication at the facility. Training users on all listed elements of above equipment. Worked with companies to develop solutions in areas of fiber design. Developing methodologies for fabrication of new and unique fiber structures, in both silicate and nonsilicate systems. Generated regular progress reports on a number of contracts and grants, as well as being an integral part of the efforts to bring in further grants and contracts. Created and maintained the measurements lab, including preform and fiber profiling systems. Guest lectured in the department of Electrical Engineering. Advised and supervised the projects of other postdoctoral, graduate, and undergraduate students. Advisors: Dr. R. H. Stolen and Dr. Gary Pickrell.

Summer 2001-Fall 2003:

Consultant for Lambda Instruments. Consulted in the design and fabrication of specialty fibers. Preforms were mostly fabricated through modified chemical vapor deposition, including some which were polarization maintaining. Supervisor: Jon Greene.

Spring 1996-Fall 1998:

Masters Research specializing in the thermal poling of fused silica and its application in waveguide systems. Also acted as teaching assistant in undergraduate level courses (Laser Systems and Radiometry and Detection). University of Rochester. Advisor: Dr. S.N. Houde-Walter.

Summer 1994-May 1995:

Research: Testing the Density of States Model for Quantum Fields with Unbounded Action.

Testing was accomplished through modeling with finite element analysis of a system with periodic boundary conditions. Vassar College. Funded by a Starr Fellowship. Supervisor: Dr. Eric Myers.

Aug. 1993- April 1994:

Research Assistant: Variations in Ice Thickness, Gravity, and Radial Deformation in Greenland and Antarctica, Vassar College. Supervisor: Dr. Andrew Trupin.

Summer 1993:

Research Assistant/Technician: Medium Energy Group, Alternating Gradient Synchrotron, Brookhaven National Laboratory, Upton, NY. Supervisor: Dr. Robert Chrien.

Summer 1991 & 1992:

Research Assistant/Technician: Plasma Fusion Center, Alcator C-Mod Fusion Reactor, Massachusetts Institute of Technology. Supervisor: T.C. Hsu.

### **Publications:**

- Patent application on random hole optical fibers submitted to US Patent Office.
- D. Kominsky, G. Pickrell, R. Stolen, and J. I. Kim, "Pressure Sensitivity in Random Hole Optical Fibers," Submitted to Optics Letters (2004)
- G. Pickrell, D. Kominsky, R. Stolen, J. Kim, F. Ellis, A. Safaai-Jazi, and A. Wang, "Microstructural Analysis of Random Hole Optical Fibers," Photonics Technology Letters **16**, 2 (2004)
- D. Kominsky, G. Pickrell, and R. Stolen, "Generation of Random Hole Optical Fiber," Optics Letters **28**, 16 (2003)
- G.R. Pickrell, D. Kominsky, R. H. Stolen, A. Safaai-Jazi, R.G. May, and A. Wang, "Novel Techniques for the fabrication of holey optical fibers", SPIE October 28-November 2, 2001 Conference Proceedings
- D. Kominsky and R. Stolen, "Crucible Technique for Producing a Silica/Lead Indium Phosphate Hybrid Fiber," Optics in the Southeast October 4-5, 2001 Conference Proceedings
- D. Kominsky and R. Stolen, "High-nonlinearity glasses in holey fibers," Opto-Southeast September 18-19, 2000 Conference Proceedings
- with R. Michaels, et al., " $K^+$ Nucleus Scattering at 720 MeV/c," presented at the Annual Meeting of the American Physical Society, Division of Nuclear Physics, Alisomar, California. October 1993
- T. C. Hsu, A.E. Hubbard, D. Kominsky and I.H. Hutchinson, "Quasioptical Transmission System for ECE Measurements on Alcator C-Mod," presented at the 8<sup>th</sup> International Workshop on Electron Cyclotron Emission and Electron Cyclotron Heating. Gut-Ising, Germany; Published in Conference Proceedings, October 1992

### **Current Research:**

Developing and testing novel varieties of optical fibers including the random hole optical fiber. Numerous fibers have been fabricated using a number of different methodologies, including the use of In Situ Bubble Formation and sol-gel glass clad fibers. Further analysis of these fibers is ongoing, but preliminary data indicates that these materials exhibit many of the properties found in ordered hole optical fibers, such as reduced mode behavior, in large core diameter fibers. These fibers also pose great potential for a host of sensing and active component applications.

Also under development and test are fibers generated via the crucible technique. This is a method devised by myself for incorporating materials which are generally considered inimical into a single fiber. The materials often have vastly different melting temperatures and coefficients of thermal expansion. Among the materials this has been accomplished with are a Lead Indium Phosphate glass, an Erbium doped phosphate glass, both in silica hosts, and a pure tellurium oxide glass in a borosilicate host. These fibers show great promise for use in the fields of nonlinear optics and for their extremely high Raman gain potential.

**Other Research Areas of Interest:**

Theoretical and experimental investigation of the use of thermal poling to induce a second order nonlinearity in fused quartz glasses. By subjecting certain varieties of glass to a strong electric field, while simultaneously activating the glass through either thermal or optical excitation, one can create in the glass a permanent second order nonlinear susceptibility. Some of the specific areas which I worked on in this field include theoretical treatment of the origin of the nonlinearity. I also was involved in developing possible device applications which utilize this property, and possible methods for patterning the nonlinearity for device creation.

**Honors & Awards:**

May 1994      Recipient of the Ethel Hickox Pollard Memorial Physics Prize, Vassar College.

May 1995      Recipient of the Lucy Kellogg English Physics Prize, Vassar College.